Title
Programmed cell death along the midline axis patterns ipsilaterality in gastrulation

Journal
Science, 367(6474)

ISSN
0036-8075

Authors
Maya-Ramos, Lisandro
Mikawa, Takashi

Publication Date
2020-01-10

DOI
10.1126/science.aaw2731

Peer reviewed

Published in final edited form as:

Science. 2020 January 10; 367(6474): 197–200. doi:10.1126/science.aaw2731.

Programmed cell death along the midline axis patterns ipsilaterality in gastrulation

Lisandro Maya-Ramos[1], **Takashi Mikawa**[1,*]

[1]Cardiovascular Research Institute, University of California, San Francisco. San Francisco, California 94158.

Abstract

Bilateral symmetry is the predominant body plan in the animal kingdom. Left and right side cells remain compartmentalized on their ipsilateral side throughout life, but with occasional variation as evidenced by gynandromorphs and with human disorders. How this evolutionarily conserved body plan is programmed remains a fundamental yet unanswered question. Here we show that germ-layer patterning in avian gastrulation, is ipsilateral despite cells undergoing highly invasive mesenchymal transformation and cell migration. Contralateral invasion is suppressed by extracellular matrix (ECM) and programmed cell death (PCD) along the embryonic midline. Ipsilateral gastrulation was lost by midline ECM and PCD inhibition but restored with exogenously-induced PCD. Our data support ipsilaterality as an integral component of bilaterality and highlight a positive functional role of PCD in development.

One Sentence Summary:

Midline cell death establishes left-right body compartments.

Bilaterians possess two symmetrical sides and constitute 99% of all animal species (1). Human disorders and naturally occurring bilateral gynandromorphs reveal that progenitor cells of left and right sides give rise to cells that will primarily remain on the same (ipsilateral) side of the organism (2, 3). Although this topological cell fate restriction is evolutionarily conserved across many animal species, ipsilaterality is not well understood (4). It is particularly intriguing how left-right cellular mixing is prevented in birds and mammals, considering that in these species, gastrulating cells undergo an epithelial-mesenchymal transition (EMT), resulting in highly migratory and invasive mesenchymal cells (5).

Using the chick model system, we analyzed gastrulation cell movement patterns via whole-embryo live imaging. The chick allows for high precision control of spatiotemporal transfection parameters. The primitive streak (PS) is the conduit for germ layer formation and defines left-right compartments in the embryo. Fluorescently tagged left and right

*Correspondence to: takashi.mikawa@ucsf.edu.

Author contributions: TM and LMR conceptualized the project and wrote the manuscript. LMR performed all experiments.

Competing interests: Authors declare no competing interests.

Data and materials availability: All data is available in the main text, supplementary materials and Auxiliary files.

epiblast cells moved towards the PS and underwent EMT (Fig. 1A, 1B, S1A-C and movie S1), with the vast majority of ingressed cells migrating away from the PS to the ipsilateral side of transfection (left 96.1±1.2%, right 96.1±0.3%, p=0.9123, n=14) (Fig. 1C) (6). There is minimal mixing between left and right mesenchymal populations, effectively creating two compartments and patterning the ipsilateral sides.

To assess whether ipsilateral gastrulation is governed by inherent epiblast cell information or by non-cell autonomous forces, an epiblast segment from GFP transgenic chick was grafted to the contralateral side of a stage-matched wild type (WT) embryo (Fig. S1D, S1F). In a cell autonomous process, donor cells grafted isochronously at a contralateral side would be expected to move back to their originating side. However, grafted implants displayed ipsilateral gastrulation, identical to control grafts (heterotopic 91.3±4.7%, homotopic 91±2.4%, p=0.9893, n ≥ 3) (Fig. S1F, S1G, S1H). These data point to an environmentally regulated process.

In both GFP tagged and grafted embryos, labeled epiblast cells migrated without detectable obstruction until reaching the PS midline; where a sharp boundary was formed by their distribution along the PS, as if a midline barrier was preventing their movement (Fig. 1B and S1B, S1E, S1G). This precise movement restriction hinted at a midline-specific program deterring cell crossing.

To examine the midline in depth, epiblast cells were tagged with membrane-tethered GFP for multiphoton live imaging. Results showed increased apoptotic cellular membrane blebbing as cells approached the midline, (Fig. 1H, S2Q and movie S2) consistent with our previous report (7) TUNEL assay and cleaved caspase 3 immunofluorescent (IF) staining revealed broad epiblast PCD distribution in early gastrulation that became enriched at the midline in later stages (Fig. 1D and Fig. S2).

Midline PCD did not follow classical scavenger cell mediated cellular corpse clearance (8, 9) as continued presence of PCD at the midline was morphologically evident (Fig. 1E-G and Fig. S2 and S3). Together, these data indicate that PCD is enriched and persistent at the midline. Thus, we suspected midline PCD could be acting as a barrier, directing ipsilateral gastrulation.

To test this hypothesis, the ontogeny of midline PCD was traced with the early apoptosis reporter Annexin V (10). YFP-tagged secreted Annexin V was preferentially detected at the midline in cells undergoing blebbing compared to lateral epiblast (Fig. S2R, S2S and movie S4). Additionally, epiblast cells labeled with Alexa Fluor 488-conjugated Annexin V, revealed that PS midline cells undergoing PCD originate in PS posterior region (Fig. 2A-C, movie S4). Therefore, to suppress midline PCD the molecular pan-caspase inhibitor P35 was introduced posteriorly (Fig. 2D) (11). In embryos electroporated with P35:2A:H2B-GFP at the posterior region and H2B:RFP at lateral epiblast, many RFP+ cells invaded the contralateral side (36.0±1.0%, p<0.0001 n=4) (Fig. 2E-G, Fig. S4, and movies S5, S6). In comparison, lateral epiblast expressing P35 ingressed identically to WT cells (Fig. S5). Together, these results strongly suggest that midline PCD is required for ipsilateral gastrulation.

We surveyed several factors that could be involved in directing ipsilateral gastrulation (Fig. S6). FGF and Eph signals are prominent in other midline systems, yet FGFR1-FGF8 and Eph3-EphrinB1 did not mimic the PCD midline barrier function (Fig. S7) (12, 13). Therefore, we examined the ECM, which can suppress cellular movement and be involved in PCD (14, 15). Although the ECM was highly fenestrated in the lateral PS, it was uniquely enriched along the PS midline (Fig. 3A, 3C, 3D). Inversely, the membrane-bound matrix metalloproteinase 15 (MMP-15) had more expression in the lateral PS than midline PS (Fig. 3B and Fig. S8). This complementary expression pattern suggested an ECM regulation by MMP-15.

To test the role of ECM in ipsilateral gastrulation, laminin was depleted with laminin subunit alpha-1 (LAMA1) morpholino (Fig. 3I and S9). The resulting embryos exhibited higher contralateral invasion than scrambled morpholino controls (21.8% vs 4.3% , p=0.0029, n=6, n=3) (Fig. 3J, 3L and movie S7). As there was more contralateral invasion after caspase 3 inhibition, we suspected that additional ECM proteins were involved in preventing contralateral invasion (Fig. 3E, 3F). Indeed, introduction of MMP-15:2A:mCherry largely diminished midline ECM (Fig. 3I, 3G, 3H and Fig. S4) leading to robust contralateral invasion of GFP+ lateral cells (39.3±1.5% p<0.0001, n=3) (Fig. 3K, 3L and movie S8). Together, the data point to a spatial regulation of ECM enrichment along the midline, necessary for ipsilateral gastrulation.

Because the above data suggested that both PCD and ECM are required for ipsilateral gastrulation patterning, we suspected a potential interplay between these signaling axes (Fig. 4A). Midline ECM was apparent before PCD (Fig. S10A-K). Furthermore, P35-mediated PCD inhibition did not diminish midline ECM expression (Fig. S10L-O). In contrast, LAMA1 morpholino-mediated midline laminin knock-down decreased the amount of cleaved caspase 3 signal at the midline (Fig. 4B). Given that PCD occurs throughout the embryonic disc and that midline PCD originates in cells from the posterior PS, ECM may be required for the alignment of PCD along the midline, although we cannot rule out ECM as a direct PCD inducer via anoikis (14, 16). In both scenarios, we expect that the resulting atypically persisting midline PCD functions as a barrier to prevent contralateral invasion of gastrulating cells.

To directly test this possibility, we introduced PCD by two independent methods in midline laminin depleted embryos (Fig. 4C) (17, 18). Induced PCD was sufficient to locally suppress contralateral invasion, thereby restoring ipsilateral ingression in a midline ECM depleted background (Fig. 4D-F, Fig. S11, S12 and movies S9, S10). Thus, both ECM and PCD are required to pattern ipsilateral gastrulation, but only PCD is sufficient to restore ipsilaterality. In this scenario, we propose that ECM aligns PCD along the midline which prevents the contralateral invasion of mesenchymal cells thereby patterning two ipsilateral body compartments (Fig. 4G).

We have uncovered a functional and developmental role for PCD. Although developmental PCD is classically considered a process required for unnecessary cell removal and tissue morphogenesis (19), our data establishes a positive role for PCD: the patterning of ipsilateral gastrulation. Ipsilaterality could ensure a symmetrical balance by preventing large disparities

between left and right sides resulting in proper laterality development (7), viability, and fitness in bilaterians (20). These findings in the avian model will stimulate comparative work in mammals, amphibians, and other bilaterian species, as new live-imaging technologies become widely available (21). PCD is also a mechanism to curtail pathological EMT in certain malignancies (22). Our work adds another layer to this concept by showing that cellular mesenchymal migration directionality can be instructed by PCD in a physiological process.

Supplementary Material

Refer to Web version on PubMed Central for supplementary material.

Acknowledgments:

We thank E.G. Baylon, J. Hyer and T. Kornberg for their comments and assistance with statistical analysis as well as past and present Mikawa lab members for their suggestions regarding this work.

Funding: Work funded by NIH grants R01 HL122375, R37 HL078921, R01 HL132832, R01 HL148125. LMR was awarded the Howard Hughes Medical Institute Gilliam Fellowship.

References and Notes:

1. Martindale MQ, Finnerty JR, Henry JQ, The Radiata and the evolutionary origins of the bilaterian body plan. Mol Phylogenet Evol 24, 358–365 (2002). [PubMed: 12220977]
2. Happle R, Mosaicism in human skin. Understanding the patterns and mechanisms. Arch Dermatol 129, 1460–1470 (1993). [PubMed: 8239703]
3. Aw S, Levin M, What's left in asymmetry? Dev Dyn 237, 3453–3463 (2008). [PubMed: 18488999]
4. Levy V, Khaner O, Limited left-right cell migration across the midline of the gastrulating avian embryo. Dev Genet 23, 175–184 (1998). [PubMed: 9842712]
5. Thiery JP, Acloque H, Huang RY, Nieto MA, Epithelial-mesenchymal transitions in development and disease. Cell 139, 871–890 (2009). [PubMed: 19945376]
6. Mikawa T, Poh AM, Kelly KA, Ishii Y, Reese DE, Induction and patterning of the primitive streak, an organizing center of gastrulation in the amniote. Dev Dyn 229, 422–432 (2004). [PubMed: 14991697]
7. Kelly KA, Wei Y, Mikawa T, Cell death along the embryo midline regulates left-right sidedness. Dev Dyn 224, 238–244 (2002). [PubMed: 12112476]
8. Sulston JE, Horvitz HR, Post-embryonic cell lineages of the nematode, Caenorhabditis elegans. Dev Biol 56, 110–156 (1977). [PubMed: 838129]
9. Lauber K, Blumenthal SG, Waibel M, Wesselborg S, Clearance of apoptotic cells: getting rid of the corpses. Mol Cell 14, 277–287 (2004). [PubMed: 15125832]
10. van Ham TJ, Mapes J, Kokel D, Peterson RT, Live imaging of apoptotic cells in zebrafish. FASEB J 24, 4336–4342 (2010). [PubMed: 20601526]
11. Sugimoto A, Friesen PD, Rothman JH, Baculovirus p35 prevents developmentally programmed cell death and rescues a ced-9 mutant in the nematode Caenorhabditis elegans. EMBO J 13, 2023–2028 (1994). [PubMed: 8187756]
12. Tessier-Lavigne M, Goodman CS, The molecular biology of axon guidance. Science 274, 1123–1133 (1996). [PubMed: 8895455]
13. Yang X, Dormann D, Munsterberg AE, Weijer CJ, Cell movement patterns during gastrulation in the chick are controlled by positive and negative chemotaxis mediated by FGF4 and FGF8. Dev Cell 3, 425–437 (2002). [PubMed: 12361604]
14. Frisch SM, Francis H, Disruption of epithelial cell-matrix interactions induces apoptosis. J Cell Biol 124, 619–626 (1994). [PubMed: 8106557]

15. Wolf K et al., Physical limits of cell migration: control by ECM space and nuclear deformation and tuning by proteolysis and traction force. J Cell Biol 201, 1069–1084 (2013). [PubMed: 23798731]
16. Shook D, Keller R, Mechanisms, mechanics and function of epithelial-mesenchymal transitions in early development. Mech Dev 120, 1351–1383 (2003). [PubMed: 14623443]
17. Belmokhtar CA, Hillion J, Segal-Bendirdjian E, Staurosporine induces apoptosis through both caspase-dependent and caspase-independent mechanisms. Oncogene 20, 3354–3362 (2001). [PubMed: 11423986]
18. Hill RA, Damisah EC, Chen F, Kwan AC, Grutzendler J, Targeted two-photon chemical apoptotic ablation of defined cell types in vivo. Nat Commun 8, 15837 (2017). [PubMed: 28621306]
19. Meier P, Finch A, Evan G, Apoptosis in development. Nature 407, 796–801 (2000). [PubMed: 11048731]
20. Li CC, Chodirker BN, Dawson AJ, Chudley AE, Severe hemihypotrophy in a female infant with mosaic Turner syndrome: a variant of Russell-Silver syndrome? Clin Dysmorphol 13, 95–98 (2004). [PubMed: 15057125]
21. McDole K et al., In Toto Imaging and Reconstruction of Post-Implantation Mouse Development at the Single-Cell Level. Cell 175, 859–876 e833 (2018). [PubMed: 30318151]
22. Michael IP et al., ALK7 Signaling Manifests a Homeostatic Tissue Barrier That Is Abrogated during Tumorigenesis and Metastasis. Dev Cell 49, 409–424 e406 (2019). [PubMed: 31063757]
23. New, D.A.T. A new technique for the cultivation of the chick embryo in vitro. J. Embryol. exp. Morph 3, 326–331 (1955).
24. Lawson A, Schoenwolf GC, New insights into critical events of avian gastrulation. Anat Rec 262, 238–252 (2001). [PubMed: 11241193]
25. Hamburger V, Hamilton HL, A series of normal stages in the development of the chick embryo. J Morphol 88, 49–92 (1951). [PubMed: 24539719]

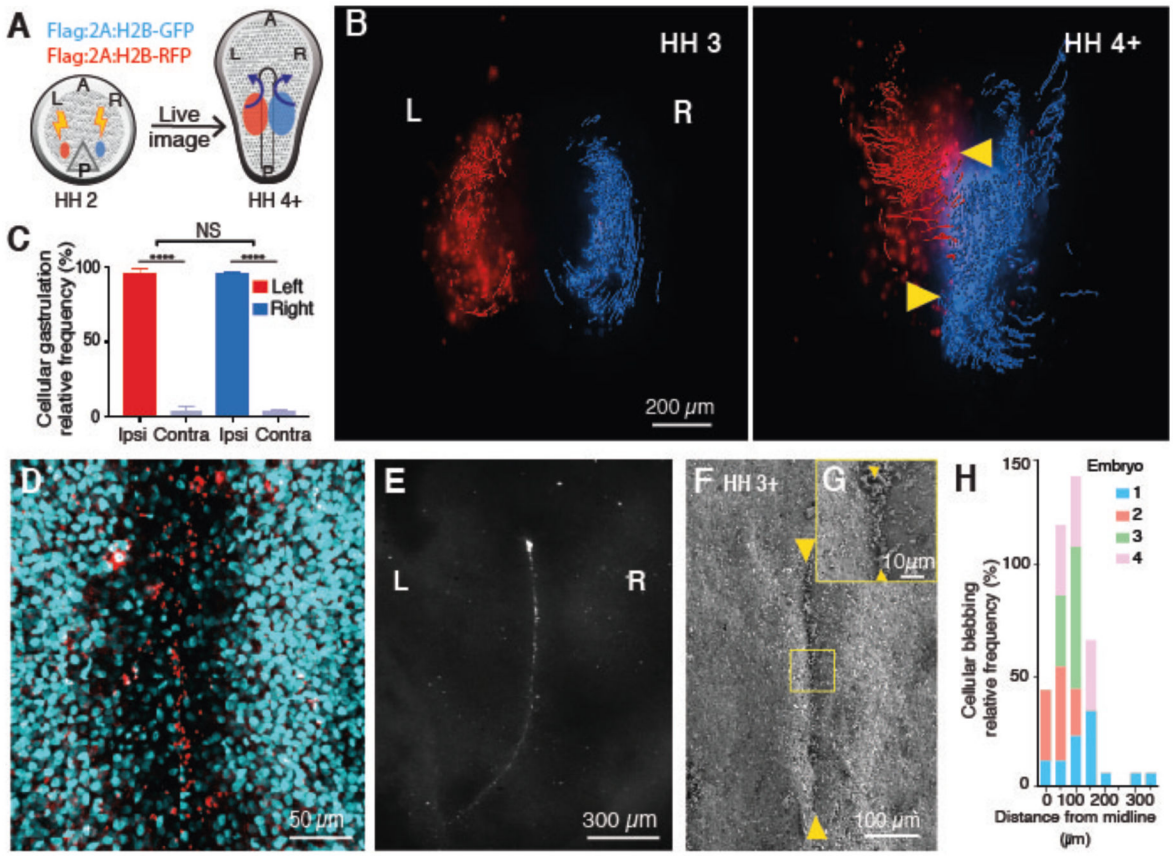

Fig. 1. Gastrulation is ipsilateral with PS midline PCD persistence.

(**A**) Experimental flow diagram. Left and right side epiblast cells were electroporated with Flag:2A:H2B-RFP (red) and Flag:2A:H2B-GFP (blue), respectively at early PS stage; tagged cells were traced during gastrulation. (**B**) Dorsal views of embryos at stages Hamburger-Hamilton (HH) 3 (25) (left) and HH4+ (right). Arrowheads, PS midline. (**C**) Ipsilateral vs contralateral distribution of tagged cells at end point. (**D**) Cleaved caspase 3+ cells (red) at the PS midline. DAPI (cyan). (**E**) Dorsal view of propidium iodide stained gastrulating embryo. Note: An array of stained cells along the PS midline. (**F,G**) SEM images of persisting cellular debris along PS midline (arrowheads). (**H**) Quantification of blebbing cells along mediolateral axis (n=4). Ipsi, ipsilateral. Contra, contralateral. A, anterior. P, posterior. L, left. R, right.

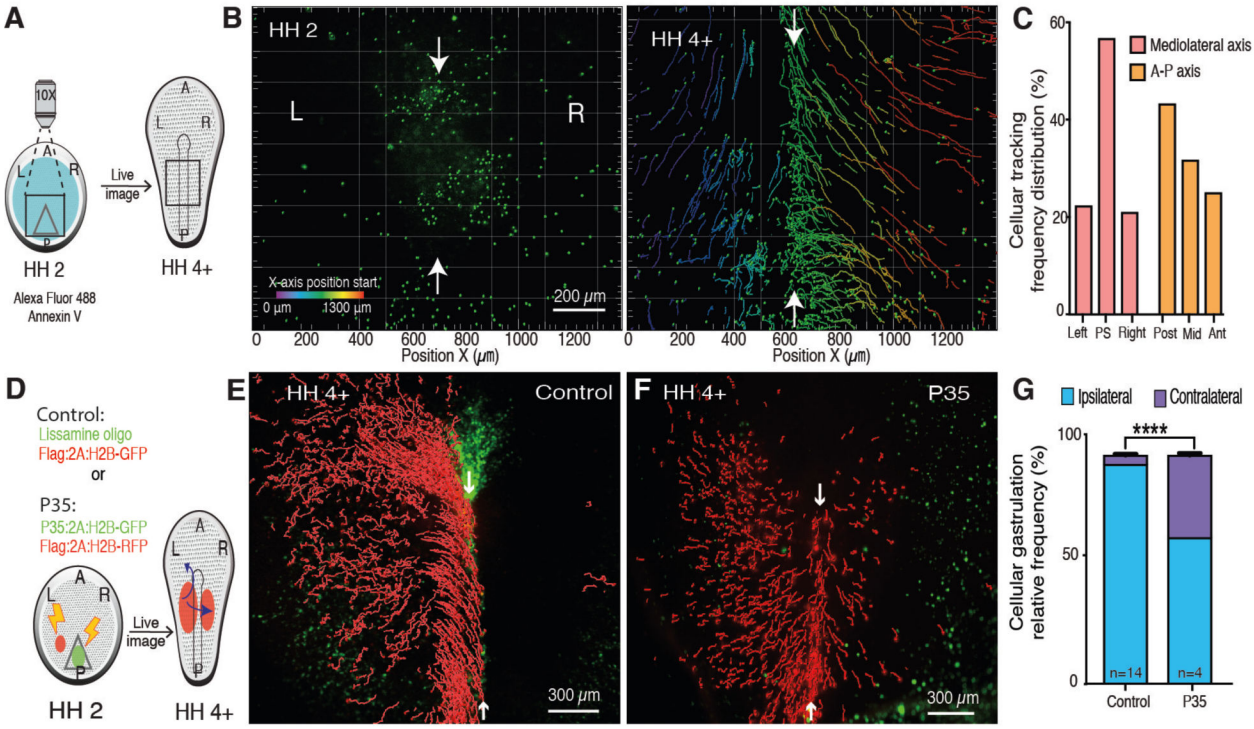

Fig. 2. PS midline PCD is necessary for ipsilateral gastrulation.

(**A**) Diagram of Annexin V epiblast cell labeling at stage HH2 and tracking to stage HH4+. (**B**) Time-lapse images of labeled cells trajectories. Color code, original X-axis position; Arrows, PS midline. (**C**) Distribution of Annexin V+ cells along the embryonic axes at HH 4+. (**D**) Diagram of control and P35 (green)-mediated midline PCD suppression with tracking of lateral epiblast cells (red) (**E**) Control ipsilateral gastrulation of H2B-GFP+ tagged cells (red) with lissamine oligo (green) along the PS (**F**) Induced contralateral invasion of H2B-RFP+ tagged cells (red) with P35 expressing cells (green) along the PS. (**G**) Quantification of P35 induced contralateral invasion. A, anterior. P, posterior. L, left. R, right.

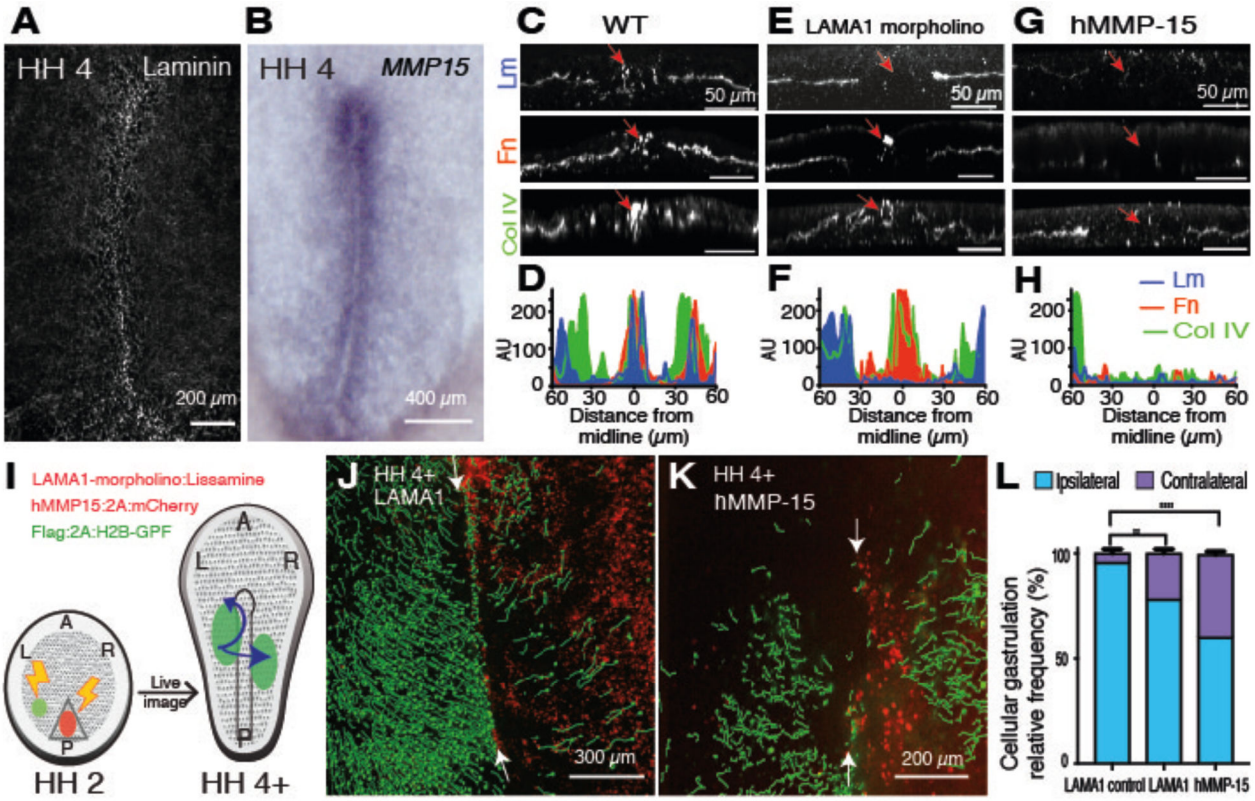

Fig. 3. PS midline ECM is necessary for ipsilateral gastrulation.

(**A**) Wholemount laminin IF staining. (**B**) Wholemount *MMP-15* in situ hybridization (ISH). (**C, E, G**) Transverse sections of HH4 WT (C), LAMA1 morpholino (E), and hMMP15 (G) treated embryos. IF staining for laminin (Lm), fibronectin (Fn) and collagen IV (Col IV). Arrows, PS midline. (**D, F, H**) Measurement of IF staining intensity of ECM proteins (indicated) at various distances from the PS midline in (C, E, G), respectively. AU, arbitrary units. (**I**) Diagram of ECM targeted proteins and subsequent gastrulation pattern analysis. (**J, K**) Induced contralateral gastrulation by LAMA1 morpholino (J) and hMMP15 (K). (**L**) Quantification of contralateral invasion. LAMA1 control morpholino (n=3), LAMA1 morpholino (p=0.0029 n=6), hMMP-15 (p<0.0001, n=3). A, anterior. P, posterior. L, left. R, right.

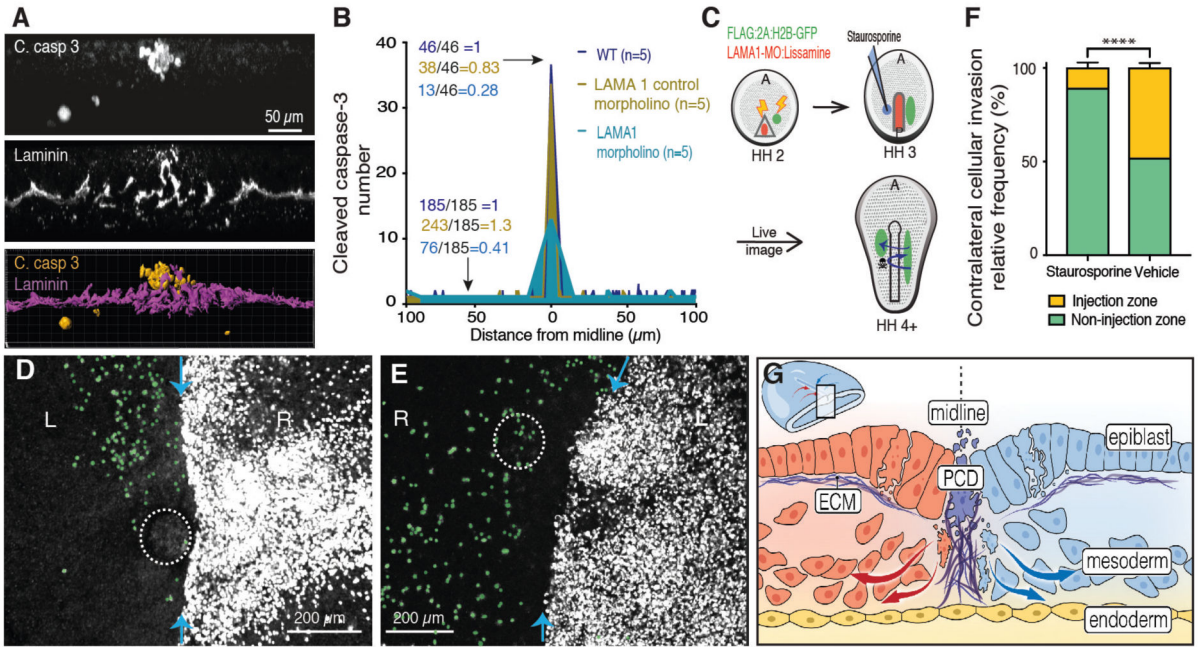

Fig. 4. Induced PCD restores ipsilateral gastrulation in ECM-depleted embryos.

(**A**) Transverse optical section, 10μm thickness, double-stained for cleaved caspase 3 (top) and laminin (middle), 3D reconstruction (bottom). (**B**) Quantification of cleaved caspase 3+ clusters at various distances from PS midline in WT embryos (yellow), control morpholino (blue) and with LAMA1 morpholino (aqua). Ratios represent total number of clusters at the midline and non-midline lateral regions. (**C**) Diagram of ipsilateral gastrulation rescue by staruosporine-induced PCD. (**D**) LAMA1 morpholino electroporated and staurosporine microinjected (dotted circle) embryo. Gastrulation pattern traced by Flag:2A:H2B-GFP (white), contralateral invading cells pseudocolored in green. Blue arrows, PS midline. (**E**) As in (D) but microinjected vehicle only (dotted circle). (**F**) Quantification of contralateral invasion suppressed by induced PCD. Injection zone vs non-injection zone (p<0.0001, n=3). (**G**) Model of PCD mediated regulation for ipsilateral gastrulation. Lm, laminin. C. Casp 3, cleaved caspase 3.